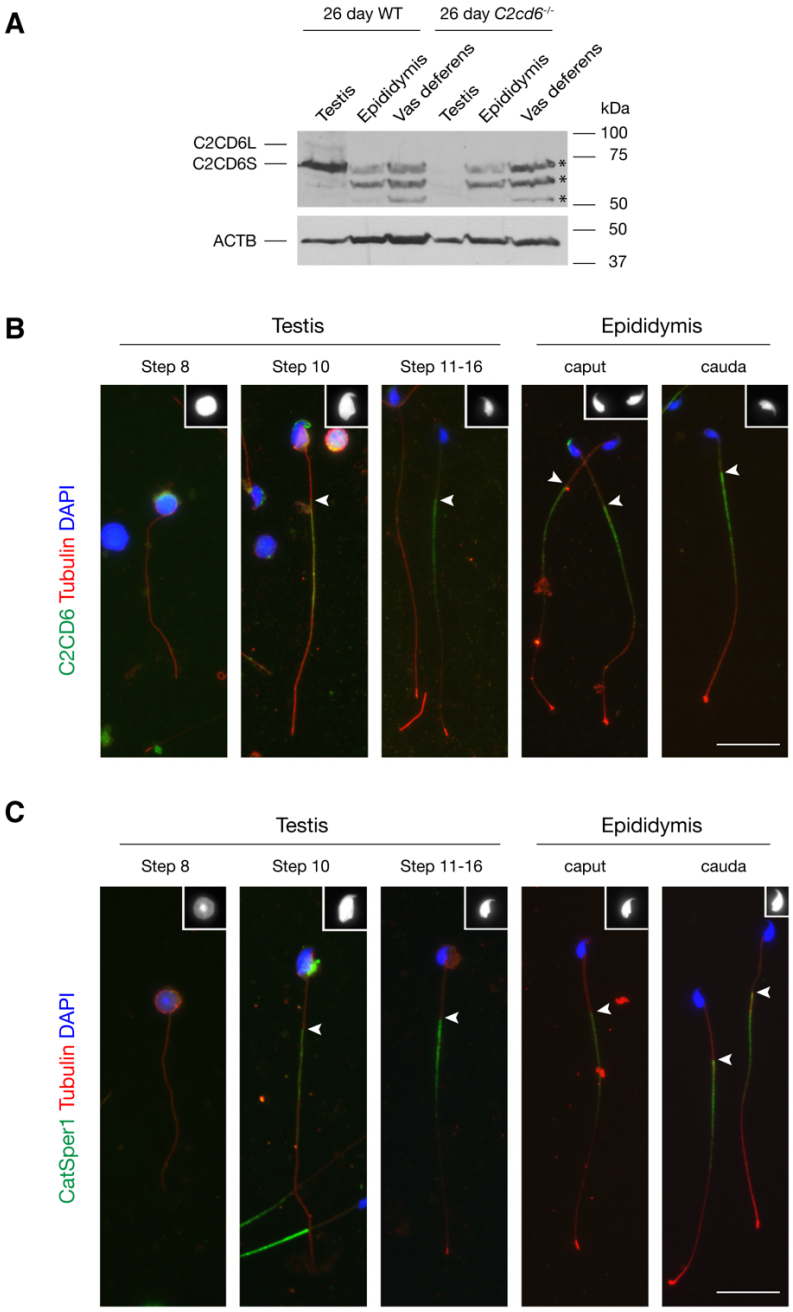

Fig. S1. Expression and localization of C2CD6 in reproductive tissues and sperm. (A) Western blot analysis of C2CD6 in testis, epididymis, and vas deferens from 26-day-old wild type and *C2cd6*$^{-/-}$ male mice. 26-day-old epididymis lacks sperm. The three bands indicated by asterisks in epididymis and vas deferens are non-specific, since they are absent in the testis but are present in the tissues from the *C2cd6*$^{-/-}$ mice. ACTB serves as a loading control. (B) Immunofluorescence analysis of C2CD6 in testicular spermatids and epididymal sperm from 8-week-old wild type mice. (C) Immunofluorescence analysis of CatSper1 in testicular spermatids and epididymal sperm from 8-week-old wild type mice. The steps of testicular spermatids are assigned based on the nuclear and flagellar morphology. Step 8 spermatid is characterized by a round nucleus and a growing flagellum. The nucleus of step 10 spermatid is wide with a hook. The nucleus of step 11-16 spermatids, like that of epididymal sperm, is condensed and narrow. Scale bars, 25 μm.

Development • Supplementary information

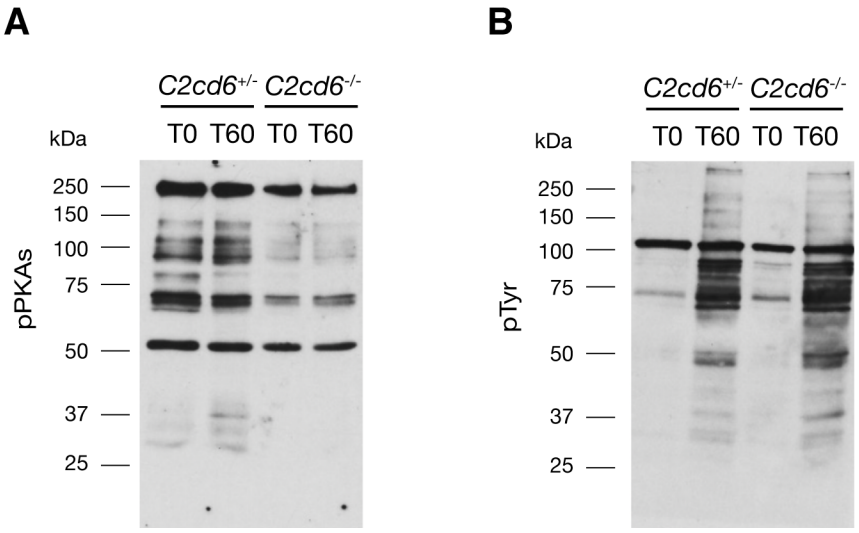

Fig. S2. Analysis of PKA phosphorylation and tyrosine phosphorylation in sperm before and after capacitation. Sperm samples from 3-to-4-month-old *C2cd6*$^{+/-}$ and *C2cd6*$^{-/-}$ males were collected immediately after swim-out (T0) and after 60 minutes of incubation in the capacitation media (T60). (A) Western blot analysis of phosphorylation of PKA substrates with phospho-PKA substrate antibody. (B) Western blot analysis of tyrosine phosphorylation with anti-pTyr antibody. The experiments were performed four times.

Development • Supplementary information

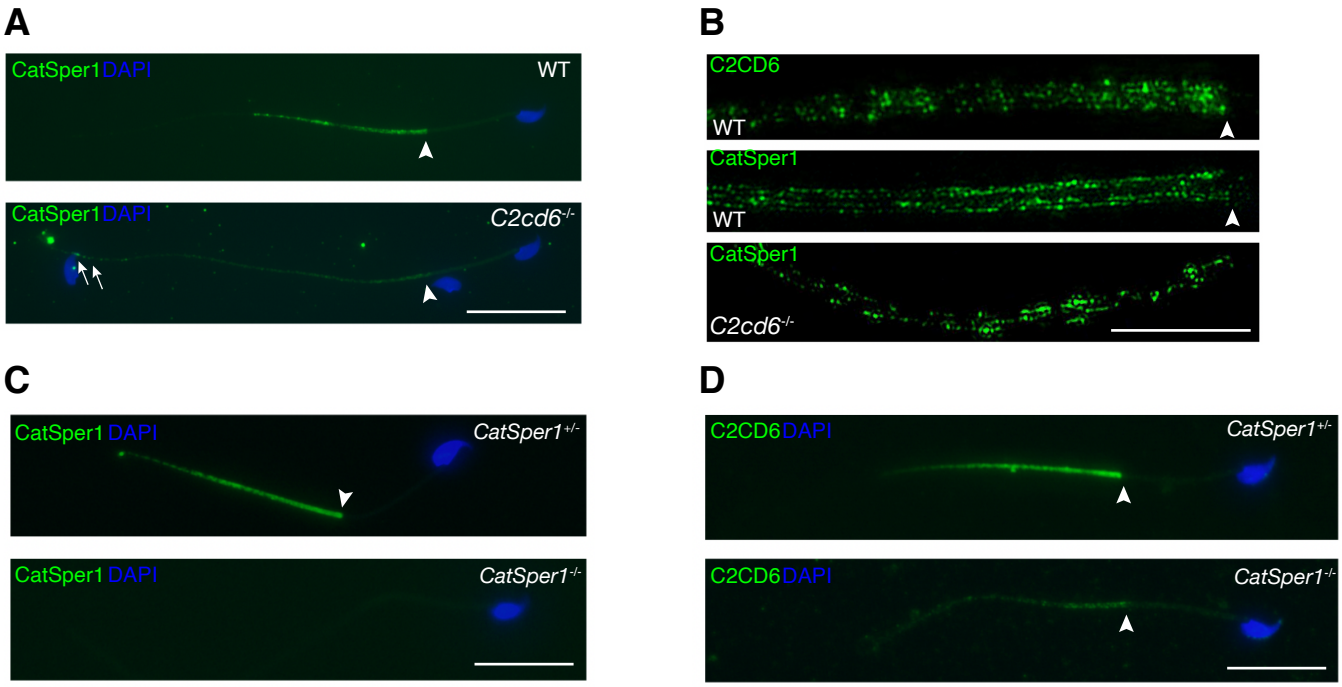

Fig. S3. Additional immunofluorescence images for Figure 4 (C2CD6 regulates targeting and nanodomain organization of CatSper in sperm flagella).

(A) Immunofluorescence analysis of CatSper1 in wild type and *C2cd6*-deficient sperm. Arrowhead indicates the annulus. Related to Fig. 4A. Scale bar, 25 µm. (B) Super-resolution localization of C2CD6 and CatSper1 in wild type and C2cd6-/- sperm. The distal region of the flagellar principal piece of the *C2cd6*$^{-/-}$ sperm is shown. Related to Fig. 4B. Scale bar, 5 µm. (C) Immunofluorescence analysis of CatSper1 in *CatSper1*$^{+/-}$ and *CatSper1*$^{-/-}$ sperm from 3-6 month-old males. Related to Fig. 4F. Scale bar, 25 µm. (D) Immunofluorescence analysis of C2CD6 in *CatSper1*$^{+/-}$ and *CatSper1*$^{-/-}$ sperm from 3-6 month-old adult males. Related to Fig. 4G. Scale bar, 25 µm.

Development • Supplementary information

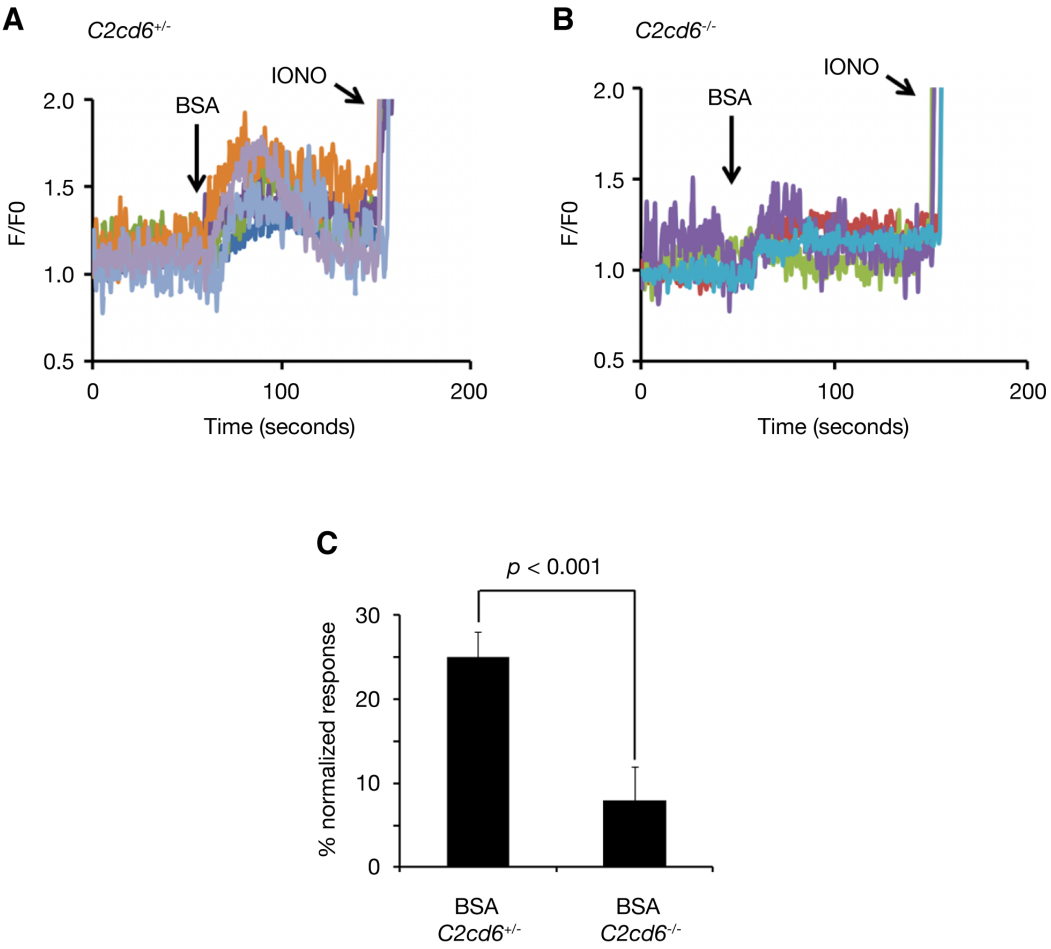

Fig. S4. BSA induces [Ca^{2+}]*i* increase in mouse sperm. (A, B) Responses in sperm calcium influx to BSA. Four to five representative single cell fluorescence traces under different experimental conditions are shown. Addition of BSA (5 mg/ml) to sperm from *C2cd6*$^{+/-}$ mice (A, five sperm) and from *C2cd6*$^{-/-}$ mice (B, four sperm). (C) The average fluorescence increases induced by BSA in 215 sperm from four different *C2cd6*$^{+/-}$ males and three *C2cd6*$^{-/-}$ males. The heterozygous sperm response is significantly larger than that of the *C2cd6*-null sperm. Statistical analysis was performed by Student's *t*-test.

Development • Supplementary information